Estimation of Entrained Water Added Mass Properties for Vibration Analysis

Donald M. MacPherson, VP Technical Director, HydroComp, Inc.
Vincent R. Puleo, Project Engineer, HydroComp, Inc.
Matthew B. Packard, Project Engineer, HydroComp, Inc.

ABSTRACT

The objective of the paper is to provide a summary survey of calculation methods that are available to estimate the entrained water properties of a propeller for vibration analysis. Ranging from simple parametric estimates to more robust predictions using radius-chord integration, the paper will present and validate calculations the axial entrained water added mass and the torsional entrained water moment of inertia.

INTRODUCTION

All mechanical systems vibrate. Sometimes these systems vibrate too much, and on occasion, bad things happen. It is the job of engineers and designers to try to ensure that bad things do not occur.

A marine propulsion engine-transmission-shaft-propeller power train is a mechanical system. It vibrates. Sometimes these systems vibrate too much, and on occasion, bad things happen. It is our job as marine engineers and naval architects to try to ensure that bad things do not occur.

How? By analyzing the vibratory properties of the system, and then comparing the results to some prescribed design criteria. A vibration analysis will look at the power train as a collection of masses, springs, dampers, and exciting loads in a variety of forms – *torsional* (rotational), *axial* (fore-and-aft), and *lateral* (shaft bending).

The aspects of vibration analysis can be found in many technical references and will not be repeated here. Rather, this paper will look at one of the small, but critical, components for the analysis – the effect of a propeller's surrounding entrained water.

VIBRATORY SYSTEM COMPONENTS

We can see the arrangement of the various components of a marine propulsion power train in the accompanying schematic illustration (Figure 1). The vibratory modes considered to be most critical are the axial and torsional, so we will limit our review to these two modes.

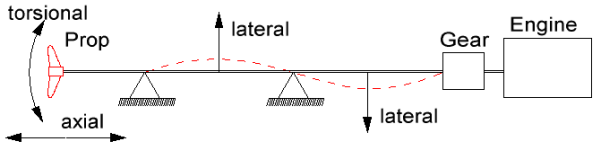

Figure 1 – Power train vibration schematic

VIBRATION COMPONENTS

The engine, transmission and propeller can be described by their individual component properties. For example, an engine is described by properties for its crankshaft and cylinders. Shafting might be described by the characteristics of the shaft cylinder and bearing points. The propeller is essentially a mass attached to the end of a beam (i.e., the shafting).

The mechanical attributes of the entire system can be calculated with relative clarity – except for the propeller and its entrained water. In fact, even the mass properties of the propeller can be found without much difficulty using direct volumetric calculations. It is the added mass and inertia of the entrained water that is the challenge to predict accurately.

PROPELLER PROPERTIES

In both axial and torsional modes, the propeller is described by two attributes – a) its volumetric mass

Available at: www.hydrocompinc.com/knowledge/
Presented to the SNAME New England Section, June 2007.

properties, and b) the water that travels with the propeller. This added mass of water is called by a variety of names, such as "wetted", "entrained" or "virtual", and is a function of the viscous (frictional) nature of water.

Axial mass properties

Let's refer to the following graphic of a propeller under axial vibration (Figure 2). As the propeller vibrates, it carries water along with it. The mass that is attached to the end of the shafting will be comprised of two parts – the mass or weight of the propeller (**W_P**) and the added mass of the entrained water (**W_E**).

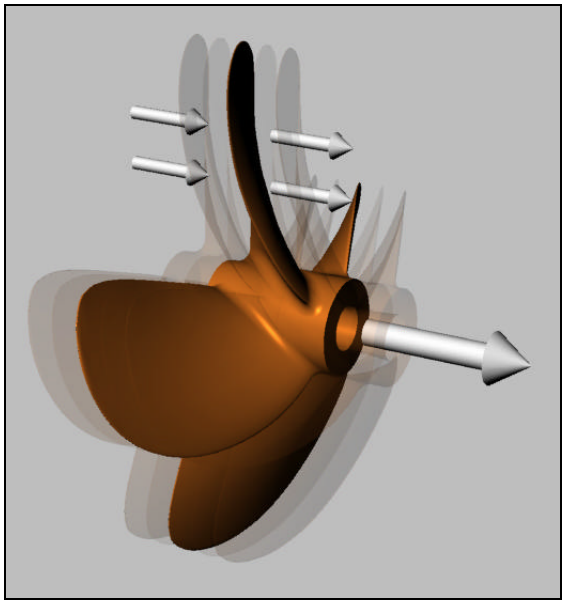

Figure 2 – Propeller added mass (axial)

Rotational considerations for the axial added mass

The axial wetted added mass, W_E, is measurably different if the propeller is locked or rotating. For clarity throughout this paper, values representing the added mass in the locked condition will have L appended (**W_{EL}**), while values for propellers in rotation will append R (**W_{ER}**).

Torsional moment of inertia properties

In the torsional mode, the propeller blades will carry some entrained water in a rotational orientation, as illustrated in Figure 3. The rotating mass, however, does not have the same effect across the entire blade, since the mass at the tip of the blade will be displaced a greater distance than at the root. Therefore, the radial "moment arm" of the position of the mass means that the property of interest is actually a torsional mass inertia at the end of the shaft. This moment of inertia of the vibrating propeller in the water is also comprised of two parts – the mass moment of inertia of the propeller (**I_P**) and the added moment of inertia of the entrained water (**I_E**).

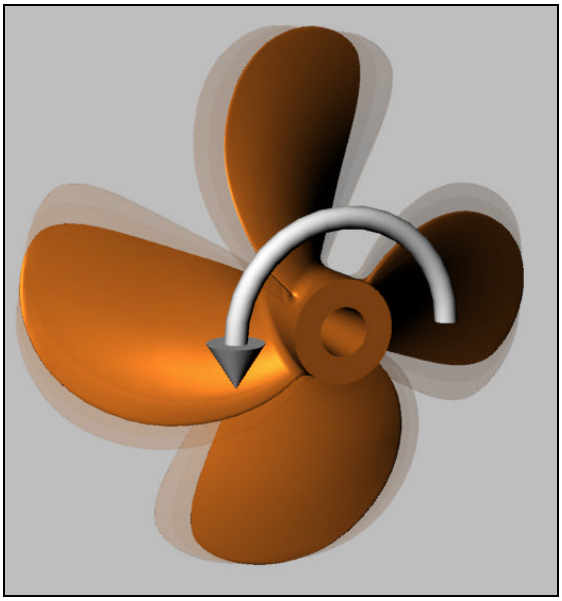

Figure 3 – Propeller added inertia (torsional)

Nomenclature

BTF = blade thickness fraction
c = blade element chord length
D = propeller diameter
DAR = developed area ratio
EAR = expanded area ratio
I_E = torsional entrained water moment of inertia
I_P = propeller material mass moment of inertia
K_I = semi-empirical wetted inertia factor
K_W = semi-empirical wetted added mass factor
K_{WL} = K_W for locked propeller (no rotation)
K_{WR} = K_W for rotating propeller
MWR = mean width ratio
P = propeller mean pitch
r = blade element radius
W_E = axial entrained water added mass
W_{EL} = W_E for locked propeller (no rotation)
W_{ER} = W_E for rotating propeller
W_P = propeller material weight
Z = number of blades
r = density of water (e.g., lb/ft^3, kg/m^3)
f = blade element pitch angle

SOURCES FOR TEST DATA OF PROPELLER PROPERTIES

Empirical test values for these properties have been hard to find. In fact, for this analysis, the authors found only two sets of data for propellers that were physically tested for their vibration-related properties.

The most extensive data was for a collection of propeller models that were tested at King's College over 40 years ago [Burrill, 1962]. About two-thirds of the nearly 50 models were from the 3-bladed KCA series (commonly known as Gawn propellers). The remaining propellers were from additional stock at King's College that included the KCC and KCD series (principally of 3 and 4 blades, but with a few 5- and 6-bladed propellers).

Also from the 1960's, the second source is a much more modest test program of seven B-series propellers [Wereldsma, 1965].

Unfortunately, no empirical test data for the axial added mass was found for the same propellers in both the locked (W_{EL}) and rotating (W_{ER}) conditions. The Burrill propellers were tested in the locked condition, while the Wereldsma propellers were rotating.

Propeller models from both of these sources are used for the validation studies in Appendix A.

SIMPLE PARAMETRIC ESTIMATES FOR PROPELLER PROPERTIES

The accurate calculation of these properties is critical for a reliable vibration analysis. An analysis using the semi-empirical radial integration method – as described later in this paper – is the recommended method to calculate these properties. However, there may be times that a vibration analysis is conducted early in the ship design cycle for which a propeller design is not yet available. In these circumstances it will be necessary to use estimates, so a representative example of a few simple parametric estimates will be described herein.

Traditional formula

A number of traditional estimate formula can be found in the technical literature. By-and-large, these are unsatisfactory for an accurate prediction of the properties. A sample of these formula include:

W_P, propeller material weight

$$W_P = K\ MWR\ BTF\ D^3$$

where, K = 0.26 for W_P in pounds and D in inches [Harrington, 1971].

This formula estimates propeller weight based on a reasonable definition of blade thickness and width, but not the number of blades or the material density. The authors believe that the formula is based on four-bladed propellers of manganese bronze. A more accurate variant of this formula might be derived to consider that approximately half of the weight is from the blades and half from the hub, as well as for differences in material density.

W_E, axial entrained water added mass

$$W_E = K\ W_P$$

where, K = 0.10 to 0.20 [VERITEC, 1985].

This rough estimate does not consider the effect of rotation or differences in propeller geometry.

I_P, propeller material mass moment of inertia

$$I_P = W_P\ D^2 / K$$

where, K = 19 to 28, with a figure of 23 often cited as a representative average.

While it is not unreasonable to base an estimate of a propeller's mass moment of inertia on its weight, there is no explicit consideration of the distribution of weight due to the blade outline. The variation of the K coefficient is intended to account for all such differences in propellers.

I_E, torsional entrained water moment of inertia

$$I_E = K\ I_P$$

where, K = 0.25 to 0.30, with a figure of 0.25 often used as a representative average [Saunders, 1957]. Other references suggest a range of 0.25 to 0.50 [VERITEC, 1985].

This is perhaps the most oft quoted traditional estimate, and perhaps is also the one with the greatest potential for error. It simply makes no sense to base the inertia of the entrained water on the inertia of the propeller material mass, and, as is shown later, the range of K is far too narrow to represent many contemporary propellers.

Parsons estimates

The following estimates for I_E and W_{ER} are based on statistical analysis of numerical calculations for B-series propellers using specialized lifting-line and lifting-surface code [Parsons, 1983]. The equation forms are:

$$I_E = C_{IE}\ LSC_{IE}\ r\ D^5$$

$$W_{ER} = C_{WER}\ LSC_{WER}\ r\ D^3$$

and, the C-factors above both follow the form:

$$C = C_1 + C_2\ EAR + C_3\ {}^{P}\!/_{D} + C_4\ EAR^2 + C_5\left({}^{P}\!/_{D}\right)^2 + C_6\ EAR\ {}^{P}\!/_{D}$$

Six coefficients are used to make up the C-factors, which are shown in the appropriate tables below. Also shown are the lifting surface correction (LSC) coefficients. A factor describing the blade's geometric aspect ratio (AR) is:

$$AR = 0.22087\ Z / EAR$$

I_E, torsional entrained water moment of inertia

C_{IE}	$Z = 4$	$Z = 5$	$Z = 6$
C_1	0.00303	0.00278	0.00237
C_2	-0.00808	-0.00716	-0.00629
C_3	-0.00407	-0.00373	-0.00306
C_4	0.00341	0.00305	0.00275
C_5	0.00043	0.00046	0.00023
C_6	0.00997	0.00853	0.00736

Table 1 – C_{IE} coefficients

$$LSC_{IE} = 0.61046 + 0.34674\ {}^{P}\!/_{D} + 0.60294\ AR^{-1} - 0.56159\ AR^{-2} - 0.80696\ {}^{P}\!/_{D}\ AR^{-1} + 0.45806\ {}^{P}\!/_{D}\ AR^{-2}$$

W_{ER}, axial entrained water added mass (rotating)

C_{WER}	$Z = 4$	$Z = 5$	$Z = 6$
C_1	-0.06295	-0.04737	-0.03913
C_2	0.17980	0.13499	0.10862
C_3	0.05872	0.04343	0.03731
C_4	0.17684	0.15666	0.13359
C_5	-0.00214	-0.00042	-0.00033
C_6	-0.15395	-0.12404	-0.10387

Table 2 – C_{WER} coefficients

$$LSC_{WER} = 0.61791 + 0.23741\ {}^{P}\!/_{D} + 0.11886\ AR^{-1} - 0.43911\ AR^{-2} - 0.46697\ {}^{P}\!/_{D}\ AR^{-1} + 0.25124\ {}^{P}\!/_{D}\ AR^{-2}$$

Schwanecke estimates

These estimates are suggested for merchant ship propellers [VERITEC, 1985] [Schwanecke, 1963]. The rotating or locked characteristic of the axial added mass, W_E, is not described in the reference, but the magnitude of the estimates suggests that it is for rotating propellers.

I_E, torsional entrained water moment of inertia

$$I_E = C_{IE}\ r\ D^5$$

$$C_{IE} = \frac{0.0703\left({}^{P}\!/_{D}\right)^2\ EAR^2}{p\ Z}$$

W_{ER}, axial entrained water added mass (rotating)

$$W_{ER} = C_{WER}\ r\ D^3$$

$$C_{WER} = \frac{0.6363\left({}^{P}\!/_{D}\right)^2\ EAR^2}{p\ Z}$$

Burrill estimates

As part of the extensive empirical testing, Burrill also developed simple estimates for the two entrained water properties [Burrill, 1962]. The data set includes the Gawn propellers, which would make these estimates applicable to the majority of inboard-driven workboats and motor yachts.

I_E, torsional entrained water moment of inertia

$$I_E = \left(C_1\ EAR\ {}^{P}\!/_{D} - C_2\right) SG \left(\frac{D}{1.33}\right)^5$$

	$Z = 3$	$Z = 4$	$Z = 5$	$Z = 6$
C_1	1.37	1.09	0.98	0.90
C_2	0.30	0.23	0.21	0.20

Table 3 – I_E coefficients

The units for the formula are for D in inches and I_E in pound-feet^2. SG is the specific gravity of the water. It must also be noted that the blade area ratio used in the original formula was the developed area ratio (DAR), but this is generally close in magnitude to the EAR as used here.

W_{EL}, axial entrained water added mass (locked)

$$W_{EL} = \left(C_1\ EAR \cos^2 q - C_2\right) SG \left(\frac{D}{1.33}\right)^3$$

	$Z = 3$	$Z = 4$	$Z = 5$	$Z = 6$
C_1	34.7	34.7	34.7	34.7
C_2	4.2	6.7	8.3	9.6

Table 4 – W_{EL} coefficients

The units and values are the same as above for W_{EL} in pounds, and θ is the pitch angle at the two-thirds radius.

Proposed new estimates

When reviewing the Burrill estimates, the authors found that in many cases, the formula did not do a

very good job at accurately estimating the properties for the propellers in the data set. So, the authors set out to developed a more general and accurate variant of the Burrill estimates, which is described below.

I_E, torsional entrained water moment of inertia

$$I_E = C_{IE}\ r\ D^5$$

$$C_{IE} = C_1\ EAR\ {}^{P}\!/_{D} - C_2$$

	Z = 3	*Z = 4*	*Z = 5*	*Z = 6*
C_1	0.00477	0.00394	0.00359	0.00344
C_2	0.00093	0.00087	0.00080	0.00076

Table 5 – C_{IE} coefficients

The fit of the proposed new coefficients to the Burrill data set is shown in Figure 4 below.

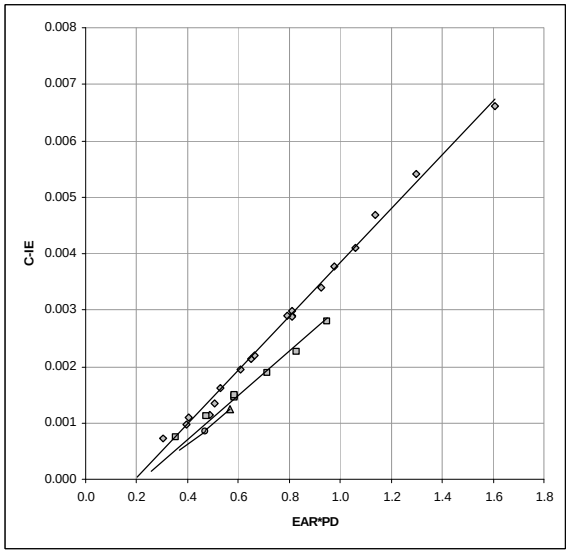

Figure 4 – C_{IE} fit to Burrill data

W_{EL}, axial entrained water added mass (locked)

$$W_{EL} = C_{WEL}\ r\ D^3$$

$$C_{WEL} = \frac{C_1\ EAR}{5 + \left({}^{P}\!/_{D}\right)^2} - C_2$$

	Z = 3	*Z = 4*	*Z = 5*	*Z = 6*
C_1	1.0638	0.9553	0.9104	0.8588
C_2	0.023	0.030	0.032	0.033

Table 6 – C_{WEL} coefficients

The fit of these proposed new coefficients to the Burrill data is shown in the accompanying Figure 5.

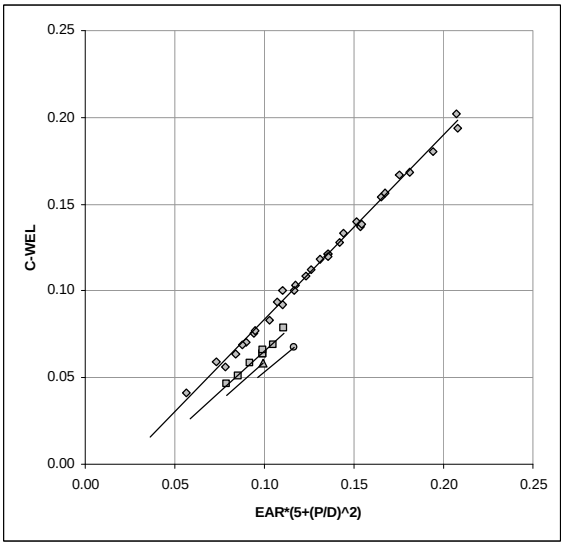

Figure 5 – C_{WEL} fit to Burrill data

W_{ER}, axial entrained water added mass (rotating)

A new relationship to correct the entrained water added mass from "locked" to "rotating" is described in a later section. This correction factor can be applied to the C_{WEL} to obtain C_{WER} as follows:

$$C_{WER} = \frac{C_{WEL}}{0.62\left({}^{P}\!/_{D}\right)^2 - 1.51\ {}^{P}\!/_{D} + 2.09}$$

CALCULATION BY RADIAL INTEGRATION OF BLADE ELEMENTS

The simplified estimates described above were all based on overall propeller blade parameters (e.g., expanded area ratio, pitch/diameter ratio), which do not consider the effect of the distribution of these parameters. For example, a blade with more of its blade area near the tip will have higher torsional inertia properties than one with its centroid of area closer to the hub.

A review of the published Burrill data indicates that changes in pitch distribution (e.g., off-loading the tip or reducing the pitch into the hub) can change W_E by as much as 5% and I_E by over 2%. (The I_E differences could be higher with different blade outlines). The effect of blade outline (i.e., the chord distribution) is even more significant for I_E due to the fact that the outer radii are more important, with variations of I_E exceeding 10%. Therefore, if an accurate prediction of these propeller properties is needed, then a more thorough geometric calculation may be justified.

A semi-empirical blade element integration calculation can provide a better analytical evaluation

of these properties. Consider the graphic of a radial slice, or *blade element*, in Figure 6 below (shown in the lighter grey color on the blade). The axial wetted added mass, W_E, will be related to the fore-and-aft projected area of the blade element. The projected area of the element is a function of the *cosine* of the element's pitch angle times the chord length. The torsional wetted inertia, I_E, on the other hand, would be related to the profile area of the element in rotation. Profile area is a function of the *sine* of the pitch angle.

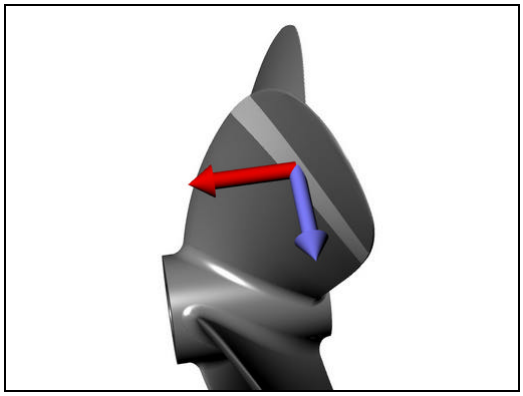

Figure 6 – Blade element radial slice

Properly integrating the blade elements will give us the geometric core of a reliable calculation methodology. The calculations can be described by

$$I_E = K_I \frac{\rho r Z}{4} \int_{r_{hub}}^{r_{tip}} (r\, c \sin j)^2 \, dr$$

$$W_E = K_W \frac{\rho r Z}{4} \int_{r_{hub}}^{r_{tip}} (c \cos j)^2 \, dr$$

where,

K_I = semi-empirical wetted inertia factor

K_W = semi-empirical wetted added mass factor

Blade element integration can be conducted by various approaches, such as Simpson's Rule or trapezoidal integration using narrow blade elements. (Our studies indicate that trapezoidal integration is quite acceptable if the radial blade elements slice width is logically defined based on curvature of the blade outline. In other words, the typical increase in curvature near the tip requires closer spacing.)

The challenge to the development of an accurate calculation, therefore, is in the definition of the K_I and K_W factors. There are few sources of published information for these factors. The authors have prepared a newly developed re-analysis of the Burrill data, as described below, for use in HydroComp's PropCad™ propeller geometric modeling software.

Kruppa K_I factor

A reference was uncovered to an equation for the wetted inertia that was noted as being from Kruppa.

$$K_I = \frac{0.952}{1 + 9.15\left(EAR/Z\right)^2}$$

The equation, modified to suit the integration format described above, is shown below. Our evaluation of this formula suggests that it will over-predict the wetted inertia by as much as 10%, and is not recommended for use.

Burrill K_I and K_{WL} factors

Burrill provided tables for estimates of both K_I and K_{WL} coefficients. (K_{WL} was noted as K_A in the reference). These factors were derived from curves fit through the test data. They were shown in tables separated by number of blades (Z) and developed area ratio (DAR).

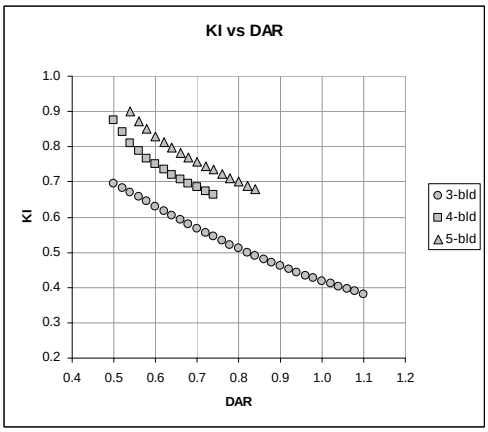

Figure 7 – Burrill K_I vs DAR

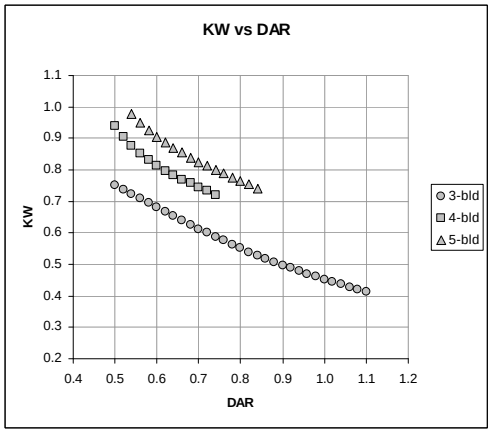

Figure 8 – Burrill K_{WL} vs DAR

Development and validation of new prediction algorithms for K_I and K_{WL} using the Burrill data

The authors conducted a new analysis of the Burrill data. The first step was to convert the data from developed area ratio (DAR) to expanded area ratio (EAR), which is more widely used in contemporary propeller analysis. The EAR was also implemented as EAR per blade, or EAR/Z, to allow for usage of the proposed factors to propellers with more and fewer blades. The range of EAR/Z was also reduced to a practical range. (Burrill had tested 3-bladed propellers with a DAR as high as 1.10, for example. A practical upper range of 0.30 for EAR/Z has been adopted for this analysis.)

While the data collapsed toward a single line, as expected, this initial analysis did reveal a curious scatter in the data. An initial curve fit was developed through these points, as shown in the plots.

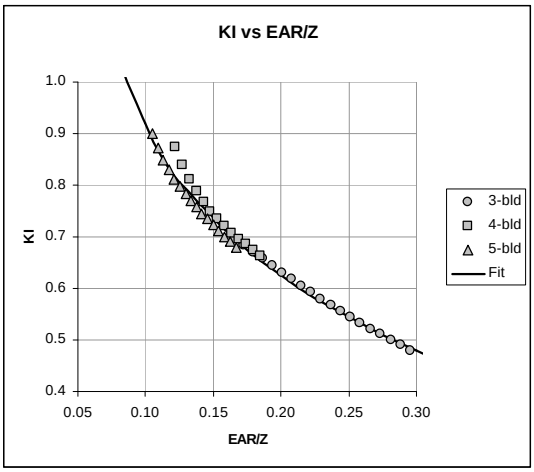

Figure 9 – Burrill K_I vs EAR/Z

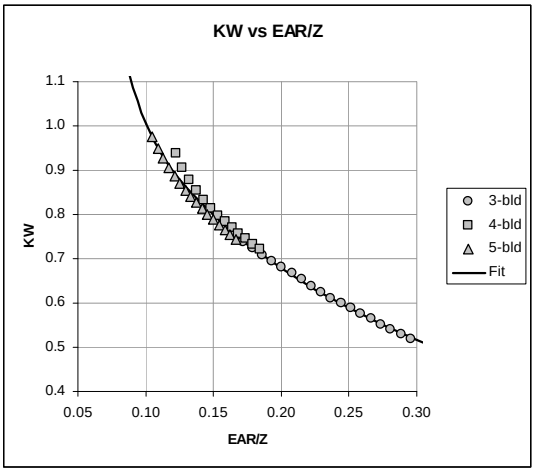

Figure 10 – Burrill K_{WL} vs EAR/Z

A sample of the Burrill propeller test results were then used to validate the curves that were fit through the data. Characteristics of these propellers are shown in the table below. The KCA propellers are a series of three-bladed ogival-section propellers with constant pitch. The KCC and KCD propellers are non-series propellers of foil section with four, five and six blades. (Some of the KCC and KCD propellers have a variable pitch distribution, so a calculated mean pitch based on chord-radius integration was used.)

Model	*Z*	*P/D*	*EAR*
KCA-306	3	0.6	0.506
KCA-410	3	1.0	0.661
KCA-112	3	1.2	0.812
KCA-116	3	1.6	0.812
KCA-216	3	1.6	1.166
KCA-208	3	0.8	1.166
KCD-11	4	0.599	0.594
KCD-4R	4	0.981	0.594
KCD-19	4	1.398	0.594
KCD-20	4	1.598	0.594
KCC-7	5	1.184	0.803
KCD-23	6	0.729	0.645

Table 7 – Burrill validation propellers

Proposed new prediction algorithm for K_I

As can be seen in Figure 11 below, there was broad scatter in the test data. (This also suggests that Burrill's fairing of the data was perhaps a bit coarse.)

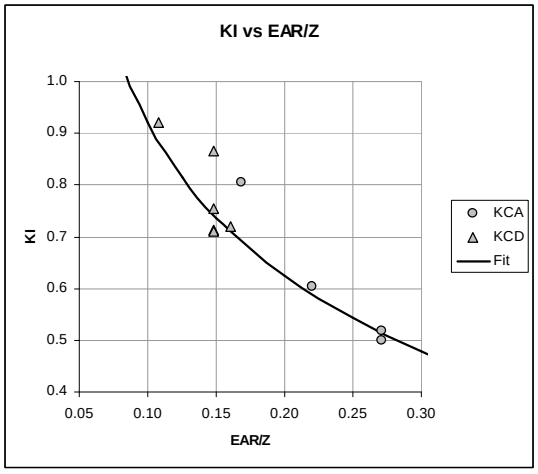

Figure 11 – Validation of K_I

Further analysis suggested that there might be a pitch/diameter contribution to K_I. A correction for pitch/diameter ratio was developed that significantly improved the prediction accuracy. Figure 12 shows the same test data with the P/D correction applied.

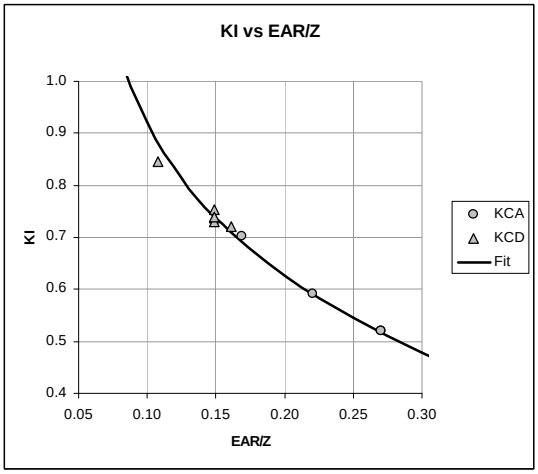

Figure 12 – Validation of K_I with P/D corr

The final form of the new prediction equation for the K_I factor, with P/D correction, is as follows:

$$K_I = \frac{1+12.47\ {}^{EAR}\!/_{Z} - 16.7\left({}^{EAR}\!/_{Z}\right)^2}{\left(22.58\ {}^{EAR}\!/_{Z}\right)\left(1.14 - \frac{0.161}{{}^{P}\!/_{D}}\right)}$$

Proposed new prediction algorithm for K_{WL}

Unlike the K_I data, the validation test propellers all very nicely fit to the fitted curve. So, no further improvement was considered.

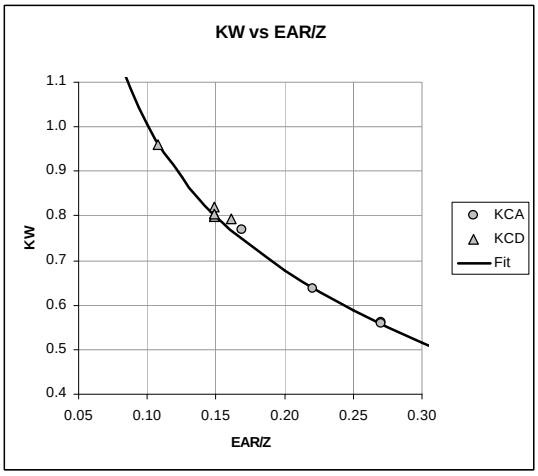

Figure 13 – Validation of K_{WL}

The proposed new prediction formula for the K_{WL} factor is as shown below.

$$K_{WL} = \frac{1+11.52\ {}^{EAR}\!/_{Z} - 15.36\left({}^{EAR}\!/_{Z}\right)^2}{19.86\ {}^{EAR}\!/_{Z}}$$

Proposed new prediction algorithm for K_{WR}

The development of a correction to account for the reduction of wetted added mass for a propeller in rotation proved quite a challenge. No propeller series were found that had been tested both rotating and locked, so a quasi-theoretical approach was followed.

A theoretical relationship between locked and rotating values [Lewis, 1960] was used as a basis, whereby the Burrill and Wereldsma test propellers were aligned to their Lewis theoretical figures. (The Burrill propellers to the Lewis "locked" value, and the Wereldsma aligned to the Lewis "rotating" value.) It was decided that a correction based on P/D might offer a logical correlation to propeller rotation. The rotating-to-locked ratio was then plotted and a curve fit to the data, as shown below in Figure 14.

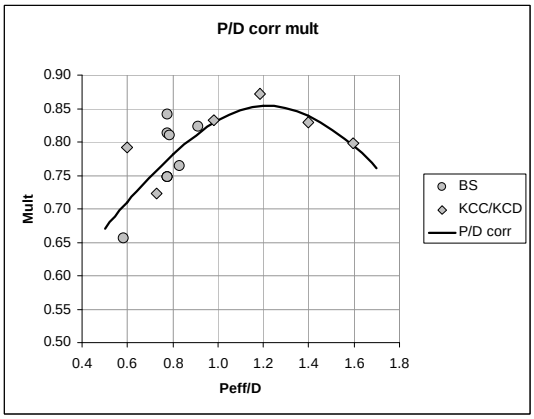

Figure 14 – Rotating-to-locked multiplier

So, the proposed new prediction formula for the K_{WR} factor, including the multiplier, is shown below.

$$K_{WR} = \frac{1+11.52\ {}^{EAR}\!/_{Z} - 15.36\left({}^{EAR}\!/_{Z}\right)^2}{\left(19.86\ {}^{EAR}\!/_{Z}\right)\left(0.62\left({}^{P}\!/_{D}\right)^2 - 1.51\ {}^{P}\!/_{D} + 2.09\right)}$$

CONCLUSIONS

New prediction formula have been proposed for both simple parametric estimates and more rigorous chord-radius integration predictions of the torsional entrained water moment of inertia and axial entrained water added mass. Both sets of new prediction methods hold the promise of improved accuracy for

vibration analysis of marine propulsion engine-gear-shaft-propeller systems.

There is room for improvement, however. The new methods somewhat over-predict I_E for 6-bladed propellers.

Perhaps the greatest opportunity for additional development is to further evaluate the contribution of section shape to the predictions. The Wereldsma B-series test results were all some 15% to 20% lower than the corresponding Burrill test results. As the proposed new methods were developed using the Burrill data, additional analysis may offer further improvement.

The Wereldsma model BS-VII shows test results that are out of place with the other test data. The model was the only 6-bladed propeller of the series and it was also expanded to a different diameter than the other propellers. Further investigation may help identify if the differences are valid, or perhaps from an error in publication or analysis.

The Shwanecke estimate of W_{ER} is substantially lower than the other estimates. An investigation of a potential publication error would be recommended.

Finally, like all proposed useful engineering utilities, these proposed new prediction methods would benefit from additional empirical test data for validation.

REFERENCES

Burrill, L.C., "Marine Propellers Blade Vibration - Full-Scale Tests", *Transactions*, North East Coast Institution of Engineers and Shipbuilders, Vol. 62, 1946

Burrill, L.C. and Robson, W., "Virtual Mass and Moment of Inertia of Propellers", *Transactions*, North East Coast Institution of Engineers and Shipbuilders, Vol. 78, 1962

Gawn, R.W. and Burrill L.C., "Effect of Cavitation on the Performance of a Series of 16 in. Model Propellers", Proceedings Spring Meeting of *Institution of Naval Architects*, 1957

Harrington, R.L., "Marine Engineering", The Society of Naval Architects and Marine Engineers, 1971

Kane, J.R., and McGoldrick, R.T., "Longitudinal Vibrtions of Marine Propulsion-Shafting Systems", *Transactions*, Society of Naval Architects and Marine Engineers, Vol. 57, 1949

Lewis, E.V., *Principles of Naval Architecture*, SNAME, 1988

Lewis, F.M and Auslaender, J.m "Virtual Inertia of Propellers", *Journal of Ship Research*, Vol. 3, No. 4, 1960

Parsons, M.G., "Mode Coupling in Torsional and Longitudinal Shafting Vibrations", *Marine Technology*, Vol. 20, No. 3, 1983

Saunders, H.E, *Hydrodynamics in Ship Design*, SNAME, 1957

Schwanecke, H., "Gedanken zur Frage der hydrodynamisch erregten Schwingungen des Propellers und der Wellenleitung", *Jahrbuch* STG, 1963

Van der Linden, C.A., 't Hart, H.H., and Dolfin, E.R., "Torsional-Axial Vibrations of a Ship's Propulsion System Part 1", *International Shipbuilding Progress*, Vol. 16, No. 173, Jan 1969

VERITEC, *Vibration Control in Ships*, 1985

Wereldsma, R., "Experiments on Vibrating Propeller Models", *International Shipbuilding Progress*, Vol. 12, No. 130, June 1965

APPENDIX A

Prediction results using the various simple estimates and detailed predictions are shown below for representative propellers from the Burrill (KCA, KCC, KCD) and Wereldsma (BS) test data.

I_E, torsional entrained water moment of inertia

Existing methods

Model	*D [ft]*	*Z*	*EAR*	*P/D*	*I_E [lb-ft^2]*	*Trad (25% I_P)*	*Parsons*	*Schwanecke*	*Burrill simple*	*Burrill chord-radius*
KCA-306	1.33	3	0.506	0.60	0.190	0.246	-	0.185	0.116	0.163
KCA-410	1.33	3	0.661	1.00	0.581	0.325	-	0.874	0.605	0.571
KCA-112	1.33	3	0.812	1.20	0.993	0.396	-	1.901	1.035	0.988
KCA-116	1.33	3	0.812	1.60	1.423	0.398	-	3.380	1.480	1.465
KCD-4R	1.33	4	0.594	0.981	0.385	0.347	0.345	0.510	0.405	0.385
KCD-19	1.33	4	0.594	1.398	0.594	0.338	0.598	1.036	0.675	0.630
KCC-7	1.33	5	0.803	1.184	0.752	0.420	0.676	1.086	0.722	0.728
KCD-23	1.33	6	0.645	0.729	0.225	0.314	0.177	0.221	0.223	0.197
Model	*D [m]*	*Z*	*EAR*	*P/D*	*I_E [kg-m^2]*	*Trad (25% I_P)*	*Parsons*	*Schwanecke*	*Burrill simple*	*Burrill chord-radius*
BS-II	6.5	4	0.596	0.776	10565	-	10161	13884	12117	11590
BS-VI	6.5	5	0.516	0.788	7912	-	6814	8585	8332	8554
BS-VII	6.25	6	0.519	0.830	5969	-	5115	6600	-	-

Proposed methods

Model	*D [ft]*	*Z*	*EAR*	*P/D*	*I_E [lb-ft^2]*	*MacPherson simple*	*Diff*	*MacPherson chord-radius*	*Diff*
KCA-306	1.33	3	0.506	0.60	0.190	0.139	-26.7%	0.187	1.6%
KCA-410	1.33	3	0.661	1.00	0.581	0.596	2.7%	0.580	0.2%
KCA-112	1.33	3	0.812	1.20	0.993	0.998	0.5%	0.984	0.9%
KCA-116	1.33	3	0.812	1.60	1.423	1.414	-0.6%	1.413	0.7%
KCD-4R	1.33	4	0.594	0.981	0.385	0.383	-0.6%	0.387	0.5%
KCD-19	1.33	4	0.594	1.398	0.594	0.645	8.5%	0.602	1.3%
KCC-7	1.33	5	0.803	1.184	0.752	0.701	-6.7%	0.740	-1.6%
KCD-23	1.33	6	0.645	0.729	0.225	0.230	2.3%	0.235	4.4%
Model	*D [m]*	*Z*	*EAR*	*P/D*	*I_E [kg-m^2]*	*MacPherson simple*	*% diff*	*MacPherson chord-radius*	*%diff*
BS-II	6.5	4	0.596	0.776	10565	11049	4.6%	12173	15.2%
BS-VI	6.5	5	0.516	0.788	7912	7655	-3.3%	9141	15.5%
BS-VII	6.25	6	0.519	0.830	5969	6884	15.3%	7501	25.7%

W_E, axial entrained water added mass

Existing methods

Model	*D [ft]*	*Z*	*EAR*	*P/D*	*W_{EL} [lb]*	*Trad (15% W_P)*	*Parsons*	*Schwanecke*	*Burrill simple*	*Burrill chord-radius*
KCA-306	1.33	3	0.506	0.60	11.21	1.7	-	-	12.0	-
KCA-410	1.33	3	0.661	1.00	13.64	2.2	-	-	14.5	-
KCA-112	1.33	3	0.812	1.20	16.62	2.6	-	-	17.0	-
KCA-116	1.33	3	0.812	1.60	13.81	2.7	-	-	13.6	-
KCD-4R	1.33	4	0.594	0.981	9.47	2.9	-	-	10.2	11.8
KCD-19	1.33	4	0.594	1.398	7.58	2.8	-	-	7.6	9.5
KCC-7	1.33	5	0.803	1.184	13.10	3.4	-	-	12.8	16.5
KCD-23	1.33	6	0.645	0.729	11.21	1.7	-	-	12.0	-
Model	*D [m]*	*Z*	*EAR*	*P/D*	*W_{ER} [kg]*	*Trad (15% W_P)*	*Parsons*	*Schwanecke*	*Burrill simple*	*Burrill chord-radius*
BS-II	6.5	4	0.596	0.776	14562	-	11588	2974	-	-
BS-VI	6.5	5	0.516	0.788	10891	-	8300	1839	-	-
BS-VII	6.25	6	0.519	0.830	7342	-	6458	1529	-	-

Proposed methods

Model	*D [ft]*	*Z*	*EAR*	*P/D*	*W_{EL} [lb]*	*MacPherson simple*	*Diff*	*MacPherson chord-radius*	*Diff*
KCA-306	1.33	3	0.506	0.60	11.21	11.7	4.4%	10.8	-3.3%
KCA-410	1.33	3	0.661	1.00	13.64	14.2	4.3%	13.7	0.3%
KCA-112	1.33	3	0.812	1.20	16.62	16.8	1.0%	16.5	-0.7%
KCA-116	1.33	3	0.812	1.60	13.81	13.8	-0.2%	13.7	-0.5%
KCD-4R	1.33	4	0.594	0.981	9.47	9.8	4.0%	9.5	0.6%
KCD-19	1.33	4	0.594	1.398	7.58	7.8	2.8%	7.6	0.5%
KCC-7	1.33	5	0.803	1.184	13.10	12.4	-5.2%	12.7	-3.4%
KCD-23	1.33	6	0.645	0.729	11.21	11.7	4.4%	10.8	-3.3%
Model	*D [m]*	*Z*	*EAR*	*P/D*	*W_{ER} [kg]*	*MacPherson simple*	*% diff*	*MacPherson chord-radius*	*%diff*
BS-II	6.5	4	0.596	0.776	14562	15231	4.6%	15281	4.9%
BS-VI	6.5	5	0.516	0.788	10891	11021	1.2%	11277	3.5%
BS-VII	6.25	6	0.519	0.830	7342	8760	19.3%	9520	29.7%